

Accepted Manuscript

Isatin-phenylhydrazone dyes and Boron complexes with large Stokes shifts:
Synthesis and Solid-State Fluorescence characteristics

Jie Zheng, Yujin Li, Yanhong Cui, Jianhong Jia, Qing Ye, Liang Han, Jianrong Gao



PII: S0040-4020(15)00455-X

DOI: [10.1016/j.tet.2015.03.115](https://doi.org/10.1016/j.tet.2015.03.115)

Reference: TET 26597

To appear in: *Tetrahedron*

Received Date: 4 December 2014

Revised Date: 17 March 2015

Accepted Date: 30 March 2015

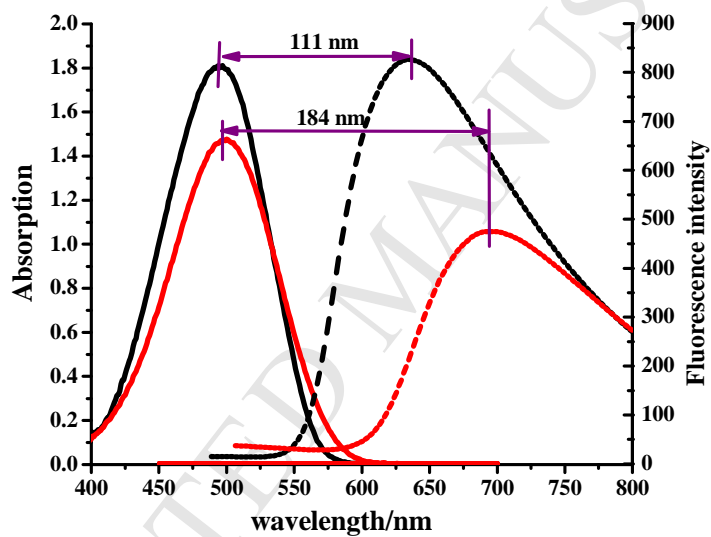
Please cite this article as: Zheng J, Li Y, Cui Y, Jia J, Ye Q, Han L, Gao J, Isatin-phenylhydrazone dyes and Boron complexes with large Stokes shifts: Synthesis and Solid-State Fluorescence characteristics, *Tetrahedron* (2015), doi: 10.1016/j.tet.2015.03.115.

This is a PDF file of an unedited manuscript that has been accepted for publication. As a service to our customers we are providing this early version of the manuscript. The manuscript will undergo copyediting, typesetting, and review of the resulting proof before it is published in its final form. Please note that during the production process errors may be discovered which could affect the content, and all legal disclaimers that apply to the journal pertain.

Graphical Abstract**Isatin-phenylhydrazone dyes and Boron complexes with large Stokes shifts:
Synthesis and Solid-State Fluorescence characteristics**

Jie Zheng, Yujin Li*, Yanhong Cui, Jianhong Jia, Qing Ye, Liang Han, Jianrong Gao**

College of Chemical Engineering, Zhejiang University of Technology, Hangzhou, 310014, P. R. China



Isatin-phenylhydrazone dyes and Boron complexes with large Stokes shifts: Synthesis and Solid-State Fluorescence characteristics

Jie Zheng, Yujin Li*, Yanhong Cui, Jianhong Jia, Qing Ye, Liang Han, Jianrong Gao**

College of Chemical Engineering, Zhejiang University of Technology, Hangzhou, 310014, P. R. China

Corresponding authors.

E-mail addresses: lyzjut@zjut.edu.cn (Y. Li).

Telephone number: +86-0571-88320891 (Y. Li).

ABSTRACT

Isatin-phenylhydrazone derivatives and their corresponding BF_2 -complexes were efficiently synthesised by a three-step reaction starting from isatin and phenylhydrazine hydrochloride. The optical properties of these isatin-phenylhydrazone derivatives and their difloroboron complexes were investigated in different organic solvens and in the solid-state. Although these fluorescent dyes exhibit feeble fluorescent intensity in solution state, high fluorescent intensity can be detected in their solid-state. The Stokes shift of these dyes can be achieved 95~198 nm vs the typical BF_2 -complexes (ca. 15 nm) in the solid-state which were caused by the remarkable geometry relaxation upon photoexcitation and its substantial effect on the energy levels of molecular orbitals. Information supporting this inference was supported by the density functional theory calculations.

Keywords: boron complexes; large Stokes shift; solid state; geometry relaxation.

1. Introduction

Difluoroboron complex fluorescent dyes exhibit high fluorescence quantum yield, excellent photostability, and sharp fluorescence spectra in solution¹ as a multipurpose fluorophore which makes they have drawn much attention in luminophores² molecular probes or molecular logic gates³ light-harvesting molecular arrays⁴ photodynamic therapy (PDT)⁵ and more recently, triplet-triplet annihilation (TTA) upconversions, etc.^{6,7} However, most boron complexes hardly fluoresce in the solid state because of the significant aggregation-caused quenching (ACQ) effect.⁸ Meanwhile, the small Stokes shift (ca. 15 nm) has never been addressed also contribute another remarkable disadvantage for the boron complexes^{9,10} which often have detrimental effects to its applications like in photoelectric conversion and electroluminescence materials¹¹ due to the emission intensity reduced by self-absorption, or the inner filter effect.^{11b,c} Thus, the boron complexes need to be decorated for the long emission and large Stokes shift in order to avoid ACQ effect for they can be used in broader fields such as field-effect transistors,¹² live-cell imaging,¹³ organic light-emitting diodes (OLEDs)¹⁴ and fluorescent sensors.¹⁵

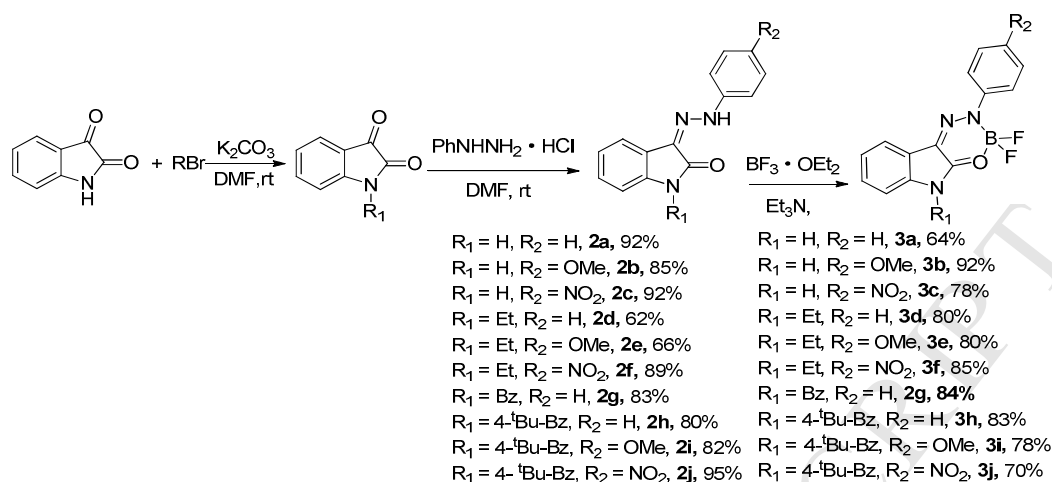
In order to address the long emission and the large Stokes shift of the boron complexes, we designed a series of new boron complexes (BODIHY) that show solid fluorescence and intrinsic large Stokes shift. These compounds show faint fluorescence in solutions, but are induced to emit intensely with the aggregate formation and the solid-state. It is noteworthy that the Stokes shift can be up to 198 nm, with excitation at green (ca. 496 nm) and emission at red (ca. 694 nm) in the solid

state. Herein, we describe the synthesis and optical properties of the BODIHY derivatives. Density functional theory (DFT) and time-dependent DFT (TDDFT) calculations have been carried out to explore the reason for the large Stokes shift of these compounds.

2 Results and discussion

2.1. Synthesis

Preparation of the substituted isatin-phenylhydrazone derivatives (precursor **2**) and their corresponding boron complexes (BODIHY **3**) is shown in Scheme 1. The N-alkylation isatin was accomplished by the reaction of isatin and alkyl bromide in the presence of K_2CO_3 (1.4 equiv.) with DMF as the solvent at room temperature. The precursor **2** was prepared by the condensation of the isatin derivative (1 equiv.) with phenylhydrazine hydrochloride (1 equiv.) in DMF at room temperature which resulted in good yield. The BODIHY **3** was produced, with a yield of 64% (**3a**), 92% (**3b**), 78% (**3c**) yield, by using an excess of $BF_3 \cdot OEt_2$ in DCM with Et_3N as the base and purification by column chromatography (silica gel, ethyl acetate: petroleum ether = 1:10). The structures of the boron complex target products **3** were characterised by FT-IR, 1H NMR, ^{13}C NMR, ^{19}F NMR, and HRMS analysis, except for the compounds **3a**, **3b**, and **3c** that are too insoluble to record a carbon NMR spectrum.



Scheme 1. The synthesis of the precursor **2** and the BODIHY **3**.

2.2. Fluorescence properties

The fluorescence properties of phenylhydrazone derivatives (**2a-2j**) and their corresponding boron complexes (**3a-3j**) were examined in different organic solvents (Fig. 1) and in their solid-states (Fig. 2). The quantum chemical calculations of the compounds **2d**, **2e**, **2f**, **2g**, **3d**, **3e**, **3f**, and **3g** at the ground state (S_0 state) and the compound **3d** at the first excited state (S_1 state) were optimized in Fig. 5 and Fig. 6. Optical data in the solution and the solid-state for all compounds are gathered in Table 1.

2.2.1. Fluorescence in solution

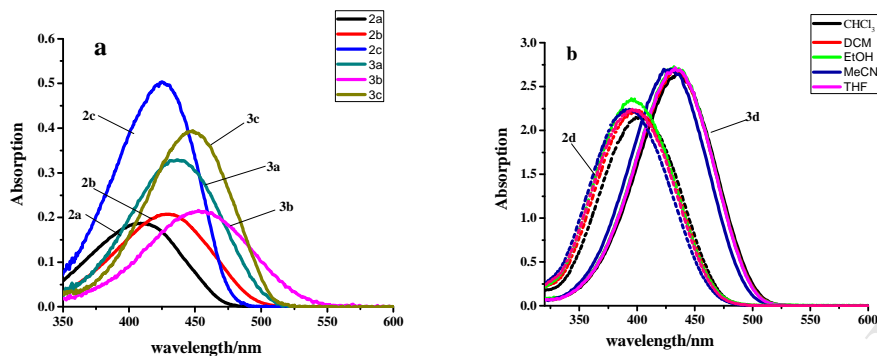


Fig. 1. (a) Absorption spectra of compound **2a**, **2b**, **2c**, **3a**, **3b** and **3c** (10 μ M) in CHCl_3 . (b) Absorption spectra of compound **2d** (dotted) and **3b** (plain) (100 μ M) in different solution.

As shown in Fig. 1 and Table 1, the precursor **2** (**2a**, **2d**, **2g**, and **2h**) with the phenyl showed a sharp absorption peak at approximately 400 nm, the precursor **2** with the p-methoxyphenyl (**2b**, **2e**, and **2i**) or p-nitrophenyl (**2c**, **2f**, and **2j**) on the arene showed the absorption peak at approximately 425 nm. The maximum absorption wavelength (λ_{max}) of BODIHY **3** (phenyl **3a**, p-methoxyphenyl **3b**, p-nitrophenyl **3c**) (437 nm, 455 nm, 449 nm) was more bathochromic than the corresponding precursor **2** (phenyl **2a**, p-methoxyphenyl **2b**, and p-nitrophenyl **2c**) (400, 425, and 425 nm). Moreover, the result also showed that it had rarely effect on the maximum absorption peak of the BODIHY **3** and precursor **2** with the different substituent on the N-atom of isatin ring (**2a**, **2d**, **2h**, **3a**, **3d**, and **3h**) (Table 1). As shown in Fig. 1 (b), the λ_{max} of these compounds were barely affected by solvent polarity, suggesting that the dipole moments of the molecules in their ground and excited states were almost equal.¹⁶ The molar absorption coefficient (ϵ) of BODIHY **3** underwent a slight change in different organic solvents (Fig. 1, Table 1) and the BODIHY **3** and precursor **2** which with the p-nitro substituted on phenyl ring had the largest value. However, the precursor **2** and BODIHY **3** hardly exhibited fluorescence in the different organic solvents which

could not be detected and the fluorescence quantum yields (Φ_f) of these compounds were below 1.00 % in the solution.

Table 1. Optical data of the precursor **2** and the BODIHY **3**.

dye	R ₁	R ₂	Matrix	$\lambda^e(\text{max})$ (nm)	ϵ (M ⁻¹ .cm ⁻¹)	$\lambda^e_{em}(\text{max})$ (nm)	Φ_f (%)	Height	Δ (nm)
2a	H	H	DCM	409	18690	578		4191	128
			solid	450					
2b	H	MeO	DCM	427	20740	622		2083	132
			solid	490					
2c	H	NO ₂	DCM	425	50400				
			solid	495					
2d	Et	H	DCM	402	21670	598		3918	113
			solid	485					
2e	Et	MeO	DCM	421	20800	628		667	133
			solid	495					
2f	Et	NO ₂	DCM	420	41100				
			solid	484					
2g	Bz	H	DCM	403	19260	584		1296	95
			solid	489					
2h	4- ^t Bu-Bz	H	DCM	396	21500	574	4.62	3018	104
			solid	470					
2i	4- ^t Bu-Bz	MeO	DCM	427	24200	614	3.28	826	111
			solid	506					
2j	4- ^t Bu-Bz	NO ₂	DCM	423	26400		< 1		
			solid	500					
3a	H	H	DCM	437	32900	636		1503	141
			solid	495					
3b	H	MeO	DCM	452	21600	694		312	198
			solid	496					
3c	H	NO ₂	DCM	449	39400	616		3309	113
			solid	503					
3d	Et	H	DCM	437	26590	646		1820	146
			solid	500					
3e	Et	MeO	DCM	455	26000	664		354	161
			solid	503					
3f	Et	NO ₂	DCM	449	54500	622		1908	126
			solid	496					
3g	Bz	H	DCM	437	23220	632		6526	134
			solid	498					
3h	4- ^t Bu-Bz	H	DCM	437	17900	656	6.10	732	163
			solid	493					

3i	4- ^t Bu-Bz	MeO	DCM	456	19700				
			solid	500		684	2.01	475	184
3j	4- ^t Bu-Bz	NO ₂	DCM	450	36700				
			solid	500		624	9.12	2428	124

λ^c : λ_{abs} for solution-state absorption or λ_{exc} for solid-state excitation of the experimental results; ϵ : the molar absorption coefficient in DCM; λ_{em}^c : the emission spectra in the solid-state of the experimental results; Δ : the Stokes shift in the solid-state of the experimental results; Φ_{F} : quantum yields in the solid-state, recorded in KBr pellets; Height: the intensity of the fluorescence in the solid.

2.2.2. Fluorescence in the solid-state

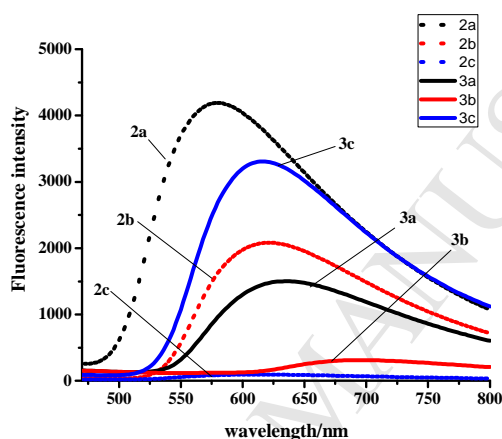


Fig. 2. Fluorescence emission spectra of the precursor **2** (dotted) (λ_{exc} = 450 nm, 490 nm, 495 nm, **2a**, **2b**, **2c**) and the BODIHY **3** (plain) (λ_{exc} = 495 nm, 496 nm, 503 nm, **3a**, **3b**, **3c**) in the solid-state (PMT Voltage: 600V).

Further, the fluorescence emission spectra of the BODIHY **3** and precursor **2** in the solid-state were measured. As shown in Fig. 2, the BODIHY **3** (phenyl **3a**, p-methoxyphenyl **3b**) had a red shift (36-83 nm) compared with the corresponding precursor **2**, for example, **2a** at 578 nm and **3a** at 636 nm, **2b** at 622 nm and **3b** at 694 nm (Table 1), and the intensity of the fluorescence of the BODIHY **3** with the p-nitrophenyl (**3c**) was much stronger than the corresponding precursor **2** (**2c**). The colour of compounds **2a**, **2b**, **2c**, **2h**, **2i**, **2j**, **3a**, **3b**, **3c**, **3h**, **3i**, and **3j** in their solid state by direct visualization and UV lamp (365 nm) are shown in Fig. 3 and it also can intuitively indicated this result. This interesting phenomenon is opposite to ACQ

effect widely observed from conventional chromophores and this aggregation-induced emission enhancement (AIEE) phenomenon have been discussed in another paper.¹⁷

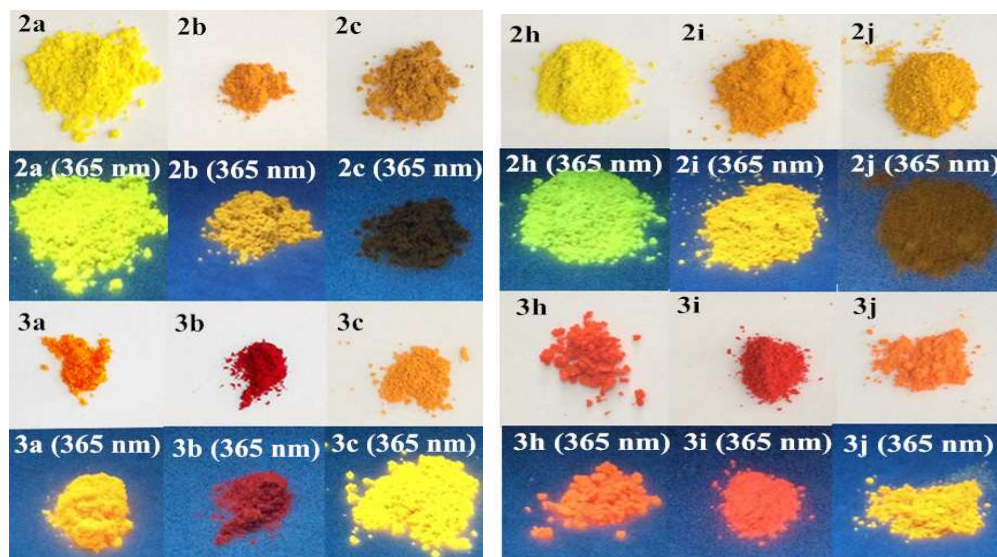


Fig. 3. The colour of compounds **2a**, **2b**, **2c**, **2h**, **2i**, **2j**, **3a**, **3b**, **3c**, **3h**, **3i**, and **3j** in the solid-state.

2.2.3. Large Stokes shift and the fluorescence quantum yield in the solid-state

As shown in Fig. 4 and table 1, both the precursor **2** and the BODIHY **3** have the large Stokes shifts which between about 95 and 198 nm in the solid-state. The maximum Stokes shift of **3b** was up to 198 nm, with excitation at green (ca. 496 nm) and emission at red (ca. 694 nm) in the solid-state. In order to investigate the effect of substituent group, a series of the precursor **2** and the BODIHY **3** with different substituent on the arene and the N-atom of the isatin ring were synthesized. Interestingly, the complexes with the different substituent on the arene change largely in the emission spectra and the Stokes shift while rarely effect can be detected with the substituent the N-atom of the isatin ring. Therefore, we chose a series of compounds **2** (**2h**, **2i**, and **2j**) and **3** (**3h**, **3i**, and **3j**) with the different substituent on

the arene to represent for the precursor **2** and the BODIHY **3** to determine the Φ_f in the solid-state. The Φ_f of the compounds (**2h**, **2i**, **2j**, **3h**, **3i**, and **3j**) in the solid-state was examined as 4.62 %, 3.28 %, <1.00%, 6.10 %, 2.01 %, and 9.12 %, respectively. For the precursor **2** (**2a**, **2d**, **2g**, and **2h**) which with the phenyl have the largest value of the Φ_f among the precursor **2**. The precursor **2** (**2b**, **2e**, and **2i**) and the BODIHY **3** (**3b**, **3e**, and **3i**) with the electron-donating group (OMe) on the arene all have the longer wavelength in the fluorescence emission spectra, and also have the larger Stokes shifts. Therefore, the electron-donating group is beneficial to the Stokes shifts of these compounds. The effect of the electron-withdrawing group (NO₂) was dramatically different for the precursor **2** and the BODIHY **3**, the precursor **2** (**2c**, **2f**, and **2j**) with the NO₂ the intensity of the fluorescence largely reduced and almost quenched in the solid-state, while the intensity of the fluorescence of the BODIHY **3** (**3c**, **3f**, and **3j**) increased to be the strongest one and has the largest Φ_f among all the compounds. Accordingly, on balance the Φ_f of the BODIHY **3** was better than the precursor **2** with the same substituent.

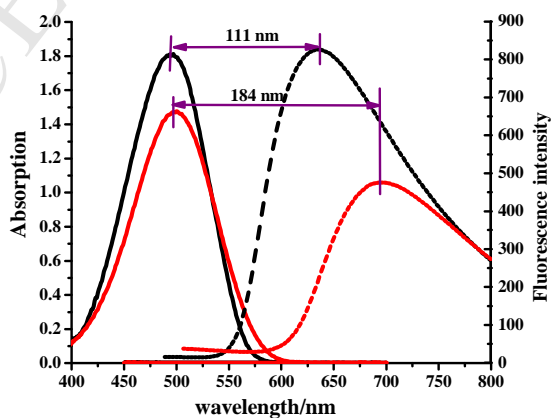


Fig.4. Absorption (plain) and emission (dotted) spectra of **2i** (black) and **3i** (red) in the solid-state.

2.2.4. Quantum chemical calculations

To better understand the photophysical properties of the precursor **2** and the BODIHY **3**, such as the UV-vis absorption and fluorescence, especially the large Stokes shift, the geometry of the compounds **2d**, **2e**, **2f**, **2g**, **3d**, **3e**, **3f**, and **3g** at the S_0 state and the S_1 state were optimized by density functional theory (DFT) and time-dependent DFT (TDDFT) methods, respectively. Revealing the photophysical properties from a theoretical perspective will be useful for the design of the substituted isatin-phenylhydrazone derivatives and their corresponding boron complexes. TD-DFT calculations have been performed at the B3LYP/6-31G(d) level of theory,¹⁸ as implemented in the Gaussian 09 program package.¹⁹ All the calculations were performed with the three-parameter functional Becke and the correlation functional of Lee et al. According to the calculated results, the UV-vis absorption spectra were simulated by Gaussian functions with the full width at half-maximum of 0.33 eV.

Table 2. The absorption spectra of **2d**, **2e**, **2f**, **2g**, **3d**, **3e**, **3f**, and **3g** of the experimental and calculated results.

dye	2d	2e	2f	2g	3d	3e	3f	3g
λ^c (max) (nm)	485	495	484	489	500	503	496	498
λ^t (max) (nm)	392	405	420	393	398	429	413	399

^cThe solid-state excitation of the experimental results. ^tThe calculated absorption.

The calculated absorption peaks of the **3d**, **3e**, and **3f** are located at 398, 429, and 413 nm, respectively (Table 2), which are consistent with the experimental results of 500, 503, and 496 nm. And the effect of the substituent group to the compounds was agreed with the experimental results. As shown in the Fig. 5, the energy gap between the HOMO and LUMO of the BODIHY **3** is **3d** (phenyl) (3.35 eV), **3e** (p-nitrophenyl)

(3.15 eV), and **3f** (p-methoxyphenyl) (3.24 eV), respectively.

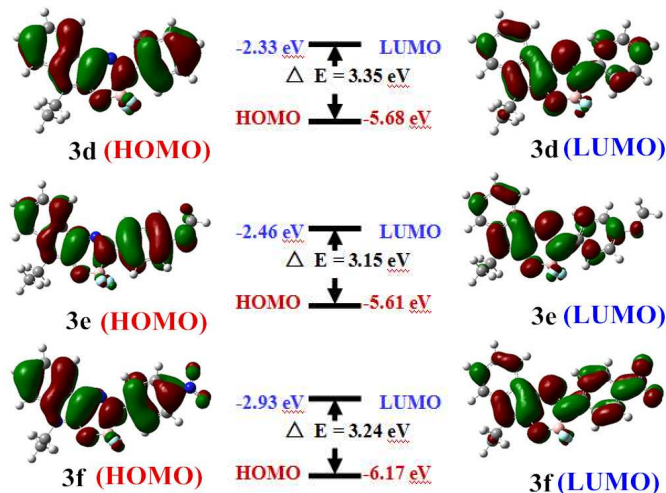


Fig. 5. Molecular orbital amplitude plots of HOMO and LUMO energy levels of **3d**, **3e** and **3f**.

In order to further research the large Stokes shift, the S_1 excited state was calculated represented by the compound **3d**. The calculated emission peak is 509 nm and the Stokes shift of the calculation is 111 nm. The calculated results were in agreement with the experimental results (146 nm). The geometry of the S_1 excited state which is responsible for the fluorescence (Kasha's rule)²⁰ is different from the S_0 state geometry (Fig. 6). The bond length of the N3-C24 in the S_1 is 1.377 Å much shorter than that in the S_0 (1.428 Å). The phenyl moiety and the BODIHY core are coplanar in the S_1 state with the dihedral angles was only 0.55° compared with that in the S_0 state (25.82 °). The geometry relaxation upon photoexcitation imparts remarkable effect on the energy level of the molecular orbitals.²⁰ For example, the LUMO is stabilized by 0.47 eV at the S_1 state geometry compared to that at the S_0 state geometry, but the HOMO is destabilized by 0.28 eV for S_1 state geometry compared to that at the S_0 state geometry. As a result, the energy gap between the

LUMO and HOMO is greatly decreased with geometry relaxation at the S_1 state compared to that at S_0 state geometry (UV-vis absorption, i.e., excitation). Thus, we propose that the geometry relaxation is the main origin of large Stokes shift for the compound **3d**, which is in agreement with the Jablonski diagram of the fluorescence.²¹

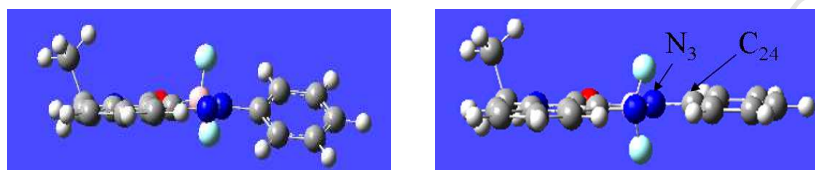


Fig. 6. The geometry of compound **3d** in the s_0 state (left) and in the s_1 state (right).

3. Conclusion

In conclusion, a new family of BF_2 -Hydrazone derivatives (**3**) containing isatin-phenylhydrazone were developed that showed enhanced fluorescence in the solid-state. These compounds exhibit weak luminescence in solution, but are highly emissive in the solid-state. All these compounds have large Stokes shift range from 95 to 198 nm. The geometries of the molecules at the S_0 state and the S_1 excited state were optimized by DFT and TDDFT, respectively. The result of the calculation of the UV-vis absorption is in agreement with the experimental result. The geometry relaxation is proposed the primary cause for the large Stokes shift of the precursor **2** and the BODIHY **3**. These series of compounds could be applied to the design of OLEDs, live-cell imaging and fluorescent sensors.

4. Experimental

4.1 General

All of the chemicals used in the current study were purchased from commercial vendors and used as received without further purification, unless otherwise noted. All solvents were purified and dried using standard methods prior to use. Fourier transform-infrared (FTIR) spectra were performed using Thermo Nicolet 6700 spectrophotometer. Nuclear magnetic resonance (^1H , ^{13}C , and ^{19}F NMR) spectra were recorded on a Bruker AM 500 spectrometer (Bruker) with chemical shifts reported as ppm at 500, 125 and 376 MHz, respectively, (TMS as internal standard). Fluorescence spectra were obtained with a F-7000 Fluorescence Spectrophotometer at solid state with PMT Voltage at 600V. UV-Vis absorption spectra were measured on a UV-2550 .

4.2 Preparation of compounds 2a-2j

A mixture of isatin (1.4722 g, 10.0 mmol), ethyl bromide (1.0905 g, 10.0 mmol) and anhydrous K_2CO_3 (2.0 g, 14.5 mmol) in DMF (10 mL) was stirred vigorously for 12 h at room temperature and complete reaction was detected by TLC analysis. The reaction mixture was poured into water (100 mL) and the precipitate was concentrated to give crude product **1a** and recrystallized from EtOH.²² A mixture of **1a** (0.8755 g, 5.0 mmol), phenylhydrazine hydrochloride (0.7325 g, 5.0 mmol) in DMF (10 mL) was stirred vigorously at room temperature overnight. The reaction mixture was poured into water (100 mL) and extracted with ethyl acetate (3 * 20 mL). The combined organic layer was dried with MgSO_4 and the solvent was removed under reduced pressure. The residue was purified by silica gel chromatography eluting (silica gel, ethyl acetate: petroleum ether = 1:5) leading to phenylhydrazone derivative **2d** as a yellow solid.²³

4.2.1. *1H-indole-3-phenylhydrazone (compound 2a)*. Yellow solid. Yield 92%. Mp 210-213 °C. ¹H NMR (500 MHz, CDCl₃): δ=12.73 (s, 1H), 7.67 (d, 2H, *J*=7.4 Hz), 7.40-7.38 (m, 4H), 7.28-7.23 (m, 1H), 7.14-7.07 (m, 2H), 6.92 (d, 1H, *J*=7.8 Hz). ¹³C NMR (125 MHz, CDCl₃): δ=163.57 (1C), 142.64 (1C), 138.15 (1C), 129.46 (2C), 128.10 (1C), 126.86 (1C), 123.42 (1C), 122.69 (1C), 122.24 (1C), 119.24 (1C), 114.52 (2C), 110.21 (1C). FTIR (KBr, cm⁻¹) 3166.0, 3057.2, 2922.3, 1681.8, 1597.0, 1556.7, 1493.0, 1463.7, 1345.5, 1296.4, 1246.2, 1171.0, 1101.2, 992.9, 859.3, 788.3, 748.8, 691.3, 628.7, 549.1, 493.4, 445.1. HRMS (ESI): calcd for C₁₄H₁₂N₃O, [M + H]⁺ 238.0980, found 238.0975.

4.2.2. *1H-indole-3-(4-methoxyphenyl)hydrazone (compound 2b)*. Deep-yellow solid. Yield 85%. Mp 185-187 °C. ¹H NMR (500 MHz, CDCl₃): δ=12.77 (s, 1H), 7.79 (s, 1H), 7.65 (d, 1H, *J*=7.6 Hz), 7.35-7.34 (m, 2H), 7.24-7.21 (m, 1H), 7.13-7.10 (m, 1H), 6.95-6.91 (m, 3H), 3.84 (s, 3H). ¹³C NMR (125 MHz, CDCl₃): δ=163.70 (1C), 156.37 (1C), 137.83 (1C), 136.48 (1C), 127.57 (1C), 125.82 (1C), 122.52 (1C), 122.41 (1C), 118.85 (1C), 115.79 (2C), 114.93 (2C), 110.17 (1C), 55.67 (1C). FTIR (KBr, cm⁻¹) 3165.2, 3057.0, 2830.5, 1674.7, 1618.6, 1592.7, 1552.6, 1519.4, 1463.1, 1388.6, 1343.3, 1299.6, 1230.2, 1175.0, 1106.2, 1040.0, 992.3, 889.7, 864.5, 822.9, 785.2, 746.5, 676.6, 538.8, 450.9. HRMS (ESI): calcd for C₁₅H₁₄N₃O₂, [M + H]⁺ 268.1086, found 268.1081.

4.2.3. *1H-indole-3-(4-nitrophenyl)hydrazone (compound 2c)*. Deep-yellow solid. Yield 92%. Mp 301-303 °C. ¹H NMR (500 MHz, CDCl₃): δ=12.90 (s, 1H), 8.28 (d, 2H, *J*=9.2 Hz), 7.70 (d, 1H, *J*=7.6 Hz), 7.60 (s, 1H), 7.44 (d, 2H, *J*=9.1 Hz), 7.34-7.31

(m, 1H), 7.18-7.15 (m, 1H), 6.94 (d, 1H, $J=7.9$ Hz). ^{13}C NMR (125 MHz, $\text{DMSO-}d_6$): $\delta=162.76$ (1C), 148.22 (1C), 141.51 (1C), 141.03 (1C), 131.73 (1C), 129.96 (1C), 125.63 (2C), 122.11 (1C), 120.47 (1C), 119.58 (1C), 113.86 (2C), 110.74 (1C). FTIR (KBr, cm^{-1}) 3298.9, 3226.2, 2433.7, 1694.3, 1603.6, 1568.1, 1506.9, 1463.2, 1329.6, 1254.0, 1206.6, 1160.4, 1108.6, 1018.0, 990.8, 888.3, 841.5, 789.3, 749.3, 688.7, 652.8, 585.8, 796.1, 448.0. HRMS (ESI): calcd for $\text{C}_{14}\text{H}_{11}\text{N}_4\text{O}_3$, $[\text{M} + \text{H}]^+$ 283.0831, found 283.0826.

4.2.4. *1-ethylindole-3-phenylhydrazone (compound 2d)*. Yellow solid. Yield 62%. Mp: 78-79 °C. ^1H NMR (500 MHz, CDCl_3) $\delta=12.83$ (s, 1H), 7.68 (d, 1H, $J=7.5$ Hz), 7.38-7.37 (m, 4H), 7.31- 7.29 (m, 1H), 7.14- 7.11 (m, 1H), 7.08- 7.05 (m, 1H), 6.93 (d, 1H, $J=7.9$ Hz), 3.89 (q, 2H, $J=7.3$ Hz), 1.35 (t, 3H, $J=7.3$ Hz). ^{13}C NMR (125 MHz, CDCl_3): $\delta=161.96$ (1C), 142.77 (1C), 140.12 (1C), 129.41 (2C), 127.94 (1C), 127.17 (1C), 123.12 (1C), 122.40 (1C), 121.54 (1C), 119.04 (1C), 114.36 (2C), 108.49 (1C), 34.19 (1C), 13.07 (1C). FTIR (KBr, cm^{-1}) 3054.3, 1973.1, 2933.3, 1677.3, 1596.4, 1563.5, 1517.5, 1466.8, 1360.3, 1249.2, 1195.0, 1126.3, 1102.2, 1053.3, 994.1, 913.6, 784.4, 746.5, 691.0, 652.3, 545.8, 500.2, 426.8. HRMS (ESI): calcd for $\text{C}_{16}\text{H}_{16}\text{N}_3\text{O}$, $[\text{M} + \text{H}]^+$ 266.1293, found 266.1288.

4.2.5. *1-ethylindole-3-(4-methoxyphenyl)hydrazone (compound 2e)*. Deep-yellow solid. Yield 66%. Mp 110-111 °C. ^1H NMR (500 MHz, CDCl_3): $\delta=12.85$ (s, 1H), 7.66 (d, 1H, $J=7.6$ Hz), 7.33-7.32 (m, 2H), 7.28-7.25 (m, 1H), 7.13 (t, 1H, $J=7.7$ Hz), 6.94-6.91 (m, 3H), 3.90 (q, 2H, $J=7.3$ Hz), 3.83 (s, 3H), 1.36 (t, 3H, $J=7.3$ Hz). ^{13}C NMR (125 MHz, CDCl_3): $\delta=162.02$ (1C), 156.18 (1C), 139.72 (1C), 136.63 (1C),

127.45 (1C), 126.07 (1C), 122.27 (1C), 121.73 (1C), 118.70 (1C), 115.62 (2C), 114.91 (2C), 108.42 (1C), 55.66 (1C), 34.17 (1C), 13.12 (1C). FTIR (KBr, cm^{-1}) 2971.1, 2934.0, 2838.4, 1673.7, 1610.6, 1562.0, 1518.9, 1466.7, 1363.8, 1296.1, 1233.9, 1125.3, 1100.0, 1038.0, 995.1, 914.0, 829.2, 783.0, 743.6, 708.2, 632.6, 538.1, 497.8, 454.2, 421.4. HRMS (ESI): calcd for $\text{C}_{17}\text{H}_{18}\text{N}_3\text{O}_2$, $[\text{M} + \text{H}]^+$ 296.1399, found 296.1394.

4.2.6. *1-ethylindole-3-(4-nitrophenyl)hydrazone (compound 2f)*. Deep-yellow solid. Yield 89%. Mp 247-249 °C. ^1H NMR (500 MHz, CDCl_3): δ =13.02 (s, 1H), 8.26 (d, 2H, J =9.3 Hz), 7.70 (d, 1H, J =7.2 Hz), 7.42-7.38 (m, 2H), 7.40-7.35 (m, 1H), 7.18-7.15 (m, 1H), 6.95 (d, 1H, J =7.9 Hz), 3.87 (q, 2H, J =7.2 Hz), 1.36 (t, 3H, J =7.3 Hz). ^{13}C NMR (125 MHz, $\text{DMSO}-d_6$): δ =163.13 (1C), 149.71 (1C), 142.70 (1C), 141.53 (1C), 132.90 (1C), 131.28 (1C), 124.84 (2C), 121.65 (1C), 119.43 (1C), 115.18 (1C), 114.48 (2C), 108.90 (1C), 33.93 (1C), 12.57 (1C). FTIR (KBr, cm^{-1}) 3545.3, 3441.0, 3250.2, 2981.4, 2942.9, 1679.2, 1599.4, 1572.3, 1499.8, 1465.3, 1378.9, 1332.3, 1264.8, 1210.5, 1164.2, 1107.3, 1052.3, 914.9, 846.4, 781.1, 754.3, 693.1, 553.1, 497.0. HRMS (ESI): calcd for $\text{C}_{16}\text{H}_{15}\text{N}_4\text{O}_3$, $[\text{M} + \text{H}]^+$ 311.1144, found 311.1139.

4.2.7. *1-benzylindole-3-phenylhydrazone (compound 2g)*. Yellow solid. Yield 83%. Mp: 138-139 °C. ^1H NMR (500 MHz, CDCl_3): δ =12.84 (s, 1H) 7.69 (d, 1H, J =7.3 Hz) 7.68-7.37 (m, 4H), 7.36-7.30 (m, 4H), 7.30-7.28 (m, 1H), 7.22-7.13 (m, 1H), 7.13-7.07 (m, 2H), 6.82 (d, 1H, J =7.9 Hz), 5.02 (s, 2H). ^{13}C NMR (125 MHz, CDCl_3): δ =162.27 (2C), 142.63 (1C), 140.18 (1C), 135.83 (1C), 129.46 (2C), 128.88 (2C),

127.96 (1C), 127.75 (1C), 127.29 (2C), 126.76 (1C), 123.29 (1C), 122.67 (1C), 121.46 (1C), 118.95 (1C), 114.42 (1C), 109.35 (1C), 43.24 (1C). FTIR (KBr, cm^{-1}) 3056.7, 3031.0, 1663.8, 1596.7, 1556.8, 1515.2, 1466.3, 1360.9, 1299.9, 1246.8, 1167.8, 1105.0, 1078.4, 1036.9, 1007.5, 785.2, 745.2, 695.1, 665.5, 627.1, 546.7, 454.6. HRMS (ESI): calcd for $\text{C}_{21}\text{H}_{18}\text{N}_3\text{O}$, $[\text{M} + \text{H}]^+$ 328.1450, found 328.1444.

4.2.8. *1-p-tert-butylbenzylindole-3-phenylhydrazone (compound 2h)*. Yellow solid.

Yield 80%. Mp 126-128 °C. ^1H NMR (500 MHz, CDCl_3): δ =12.84 (s, 1H), 7.68 (d, 1H, J =7.5 Hz), 7.41-7.35 (m, 6H), 7.28 (s, 1H), 7.27 (s, 1H), 7.25-7.20 (m, 1H), 7.13-7.11 (m, 1H), 7.09-7.06 (m, 1H), 6.87 (d, 1H, J =7.9 Hz), 4.99 (s, 2H), 1.30 (s, 9H). ^{13}C NMR (125 MHz, CDCl_3): δ =162.29 (1C), 150.76 (1C), 142.73 (1C), 140.39 (1C), 132.84 (1C), 129.44 (2C), 127.95 (1C), 127.11 (2C), 126.93 (1C), 125.78 (2C), 123.25 (1C), 122.59 (1C), 121.52 (1C), 118.94 (1C), 114.44 (2C), 109.37 (1C), 42.95 (1C), 34.53 (1C), 31.32 (3C). FTIR (KBr, cm^{-1}) 3055.7, 2960.5, 1667.4, 1596.0, 1562.7, 1508.8, 1466.6, 1353.9, 1243.4, 1164.1, 1102.2, 1034.1, 1007.8, 887.1, 784.1, 747.7, 692.1, 652.5, 547.4, 451.3. HRMS (ESI): calcd for $\text{C}_{25}\text{H}_{26}\text{N}_3\text{O}$, $[\text{M} + \text{H}]^+$ 384.2076, found 384.2070.

4.2.9. *1-p-tert-butylbenzylindole-3-(4-methoxyphenyl)phenylhydrazone (compound 2i)*.

Deep-yellow solid. Yield 82%. Mp 151-152 °C. ^1H NMR (500 MHz, CDCl_3): δ =12.87 (s, 1H), 7.66 (d, 1H, J =7.3 Hz), 7.80 (dd, 3H, J_1 =3.25 Hz, J_2 =3.30 Hz), 7.21 (t, 1H, J =7.5 Hz), 7.11 (t, 1H, J =7.3 Hz), 6.95 (d, 2H, J =1.95 Hz), 6.87 (d, 1H, J =7.8 Hz), 4.99 (s, 2H), 3.88 (s, 2H), 3.84 (s, 3H), 1.30 (s, 9H). ^{13}C NMR (125 MHz, CDCl_3): δ =162.31 (1C), 156.25 (1C), 150.69 (1C), 139.98 (1C), 136.56 (1C), 132.98

(1C), 127.44 (1C), 127.09 (2C), 125.75 (2C), 122.45 (2C), 121.69 (1C), 118.58 (1C), 115.74 (1C), 115.69 (2C), 114.92 (2C), 109.27 (1C), 55.66 (1C), 42.90 (1C), 34.53 (1C), 31.32 (3C). FTIR (KBr, cm^{-1}) 3055.0, 2959.8, 2866.1, 2843.2, 1665.3, 1610.8, 1552.4, 1517.2, 1466.1, 1358.8, 1300.6, 1239.7, 1164.4, 1101.9, 1039.6, 1008.4, 820.8, 783.8, 743.0, 713.3, 657.1, 607.2, 532.6, 451.5. HRMS (ESI): calcd for $\text{C}_{26}\text{H}_{27}\text{N}_3\text{O}_2$, $[\text{M} + \text{H}]^+$ 414.2182, found 414.2176.

4.2.10. 1-p-tert-butylbenzylindole-3-(4-nitrophenyl)phenylhydrazone (compound 2j).

Deep-yellow solid. Yield 95%. Mp 198-201 °C. ^1H NMR (500 MHz, CDCl_3): δ = 13.03 (s, 1H), 8.28-8.26 (m, 3H), 7.70-7.69 (m, 1H), 7.43-7.42 (m, 2H), 7.38-7.36 (m, 3H), 7.29-7.26 (m, 1H), 7.16-7.13 (m, 1H), 6.90-6.88 (m, 1H), 4.97 (s, 2H), 1.30 (s, 9H). ^{13}C NMR (125 MHz, CDCl_3): δ =162.20 (1C), 151.08 (1C), 147.90 (1C), 142.72 (1C), 141.54 (1C), 132.29 (1C), 130.93 (1C), 129.72 (2C), 127.15 (2C), 125.92 (2C), 125.89 (1C), 123.15 (1C), 120.55 (1C), 119.98 (1C), 114.28 (1C), 113.65 (2C), 109.84 (1C), 43.15 (1C), 34.57 (1C), 31.31 (3C). FTIR (KBr, cm^{-1}) 2962.4, 2865.7, 1734.6, 1681.1, 1603.1, 1570.2, 1505.9, 1465.8, 1331.2, 1258.1, 1151.5, 1101.6, 1032.6, 1004.6, 970.8, 845.2, 787.7, 751.5, 694.6, 630.2, 495.0. HRMS (ESI): calcd for $\text{C}_{25}\text{H}_{25}\text{N}_4\text{O}_3$, $[\text{M} + \text{H}]^+$ 429.1927, found 429.1921.

4.3 Preparation of compounds 3a-3j

To a stirred solution of **2d** (0.1328 g, 0.5 mmol) in degassed anhydrous dichloromethane (20 mL), Et_3N (1.5 mL, 10 mmol) was syringed under nitrogen atmosphere. After stirred for 20 minutes, $\text{BF}_3\cdot\text{OEt}_2$ (1.25 mL, 10 mmol) was

successively added by syringe. The mixture was stirred at room temperature overnight and complete reaction was detected by TLC. The mixture was quenched with water (20 mL), and extracted with dichloromethane (3 * 20 mL). The organic layer was dried with MgSO₄ and the solvent was removed under reduced pressure. The residue was purified by silica gel chromatography eluting (silica gel, ethyl acetate: petroleum ether = 1: 10) to afford clean complex **3d** as an orange-yellow solid.

4.3.1. 5-H-3,3-difluoro-2-phenyl-3,5-dihydro-2H-[1,3,4,2]oxadiazaborinino[6,5-b]indol-4-ium-3-uide (compound 3a). Orange solid. Yield 64 %. Mp 197-202 °C. ¹H NMR (500 MHz, DMSO-d₆): δ=13.50 (s, 1H), 7.82 (d, 1H, *J*=7.6 Hz), 7.69 (d, 2H, *J*=8.0 Hz), 7.50-7.47 (m, 2H), 7.42-7.36 (m, 2H), 7.35-7.29 (m, 2H). ¹⁹F NMR (CDCl₃, 376 MHz): δ=-130.42- -130.45 (m, 1F), -131.48- -130.51 (m, 1F). FTIR (KBr, cm⁻¹) 3376.2, 3359.5, 3066.1, 1639.4, 1592.0, 1492.3, 1458.6, 1321.2, 1297.5, 1254.3, 1194.5, 1110.8, 1043.8, 1019.6, 969.6, 894.1, 757.2, 689.3, 630.8, 574.8, 439.7. HRMS (ESI): calcd for C₁₄H₁₀BF₂N₃O Na, [M + Na]⁺ 308.0783; found 308.0785.

4.3.2. 5-H-3,3-difluoro-2-(4-methoxyphenyl)-3,5-dihydro-2H-[1,3,4,2]oxadiazaborinino[6,5-b]indol-4-ium-3-uide (compound 3b). Red solid. Yield 92%. Mp 183-185 °C. ¹H NMR (500 MHz, DMSO-d₆): δ=13.36 (s, 1H), 7.80 (d, 1H, *J*=7.5 Hz), 7.63 (d, 1H, *J*=8.8 Hz), 7.41-7.36 (m, 2H), 7.33-7.30 (m, 1H), 7.06-7.05 (m, 2H), 3.81 (s, 3H). ¹⁹F NMR (CDCl₃, 376 MHz): δ=-130.05- -130.08 (m, 1F), -131.12- -130.15 (m, 1F). FTIR (KBr, cm⁻¹) 3264.9, 3207.1, 1635.8, 1592.9, 1500.2, 11427.8, 1322.5, 1240.7, 1181.1, 1046.4, 1021.6, 973.9, 887.1, 827.3, 763.7, 557.3. HRMS (ESI): calcd for

$C_{15}H_{11}BF_2N_3O_2$, $[M - H]^+$ 314.0912; found 314.0912.

4.3.3. 5-*H*-3,3-difluoro-2-(4-nitrophenyl)-3,5-dihydro-2*H*-[1,3,4,2]oxadiazaborin-

ino[6,5-*b*]indol-4-ium-3-uide (compound **3c**). Orange solid. Yield 78%. Mp 183-185 °C. 1H NMR (500 MHz, DMSO- d_6): δ =8.35-8.32 (m, 2H), 7.90-7.85 (m, 3H), 7.47-7.44 (m, 1H), 7.38-7.34 (m, 2H). ^{19}F NMR ($CDCl_3$, 376 MHz): δ =-129.38-129.40 (m, 1F), -131.46-130.48 (m, 1F). FTIR (KBr, cm^{-1}) 3359.4, 1660.4, 1594.9, 1544.7, 1490.7, 1459.9, 1423.2, 1332.6, 1259.3, 1172.4, 1110.8, 1074.2, 1022.1, 964.2, 852.4, 775.3, 752.1, 661.5, 441.6. HRMS (ESI): calcd for $C_{14}H_8BF_2N_4O_3$, $[M - H]^+$ 329.0658; found 329.0658.

4.3.4. 5-ethyl-3,3-difluoro-2-phenyl-3,5-dihydro-2*H*-[1,3,4,2]oxadiazaborinino[6,5-*b*]

indol-4-ium-3-uide (compound **3d**). Orange solid. Yield 80%. Mp 163-166 °C. 1H NMR (500 MHz, $CDCl_3$): δ =7.90-7.88 (m, 1H), 7.85-7.83 (m, 2H), 7.47-7.44 (m, 2H), 7.40-7.39 (m, 2H), 7.39-7.36 (m, 1H), 7.35-7.26 (m, 1H), 4.19 (q, 2H, $J=7.4$ Hz), 1.53 (t, 3H, $J=7.4$ Hz). ^{13}C NMR (125 MHz, $CDCl_3$): δ =152.84 (1C), 145.16 (1C), 136.02 (1C), 128.94 (2C), 126.85 (1C), 126.54 (1C), 124.88 (1C), 123.29 (1C), 121.56 (1C), 120.72 (1C), 119.01 (2C), 110.74 (1C), 36.72 (1C), 13.45 (1C). ^{19}F NMR ($CDCl_3$, 376 MHz): δ =-130.94 (s, 1F), -131.00 (s, 1F). FTIR (KBr, cm^{-1}) 2987.2, 1608.4, 1508.5, 1321.0, 1282.5, 1210.1, 1135.9, 1023.3, 761.8, 545.8, 432.0. HRMS (ESI): calcd for $C_{16}H_{15}BF_2N_3O$, $[M + H]^+$ 314.1271, found 314.1273.

4.3.5. 5-ethyl-3,3-difluoro-2-(4-methoxyphenyl)-3,5-dihydro-2*H*-[1,3,4,2]oxadiazab-

orinino[6,5-*b*]indol-4-ium-3-uide (compound **3e**). Red solid. Yield 80%. Mp

163-165 °C. ^1H NMR (500 MHz, CDCl_3): δ =7.87 (dd, 1H, $J_1=1.4$ Hz, $J_2=1.4$ Hz), 7.80 (d, 2H, $J=9.0$ Hz), 7.37-7.34 (m, 2H), 7.28-7.25 (m, 1H), 6.97 (d, 2H, $J=3.3$ Hz), 4.17(q, 2H, $J=7.3$ Hz), 3.87 (s, 3H), 1.50 (t, 3H, $J=7.3$ Hz); ^{13}C NMR (125 MHz, CDCl_3): δ =158.84 (1C), 152.33 (1C), 138.86 (1C), 135.63 (1C), 126.06 (1C), 124.63 (1C), 122.17 (1C), 121.65 (1C), 118.74 (1C), 115.56 (1C), 114.84 (1C), 114.22 (2C), 110.61 (1C), 55.57 (1C), 36.65 (1C), 13.53 (1C). ^{19}F NMR (CDCl_3 , 376 MHz): δ =-131.66- -131.68 (m, 1F), -131.72- -131.74 (m, 1F). FTIR (KBr, cm^{-1}) 1631.5, 1500.4, 1427.6, 1322.8, 1250.4, 1212.3, 1137.5, 1023.5, 827.3, 543.8. HRMS (ESI): calcd for $\text{C}_{17}\text{H}_{17}\text{BF}_2\text{N}_3\text{O}_2$, $[\text{M} + \text{H}]^+$ 344.1376, found 344.1378.

4.3.6. *5-ethyl-3,3-difluoro-2-(4-nitrophenyl)-3,5-dihydro-2H-[1,3,4,2]oxadiazaborinino[6,5-b]indol-4-ium-3-uide* (compound **3f**). Orange solid. Yield 85%. Mp 211-215 °C. ^1H NMR (500 MHz, CDCl_3): δ =8.30-8.27 (m, 2H), 7.97 (d, 2H, $J=9.2$ Hz), 7.91 (d, 1H, $J=7.4$ Hz), 7.49-7.46 (m, 1H), 7.43-7.40 (m, 1H), 7.30-7.28 (m, 1H), 4.19 (q, 2H, $J=7.3$ Hz), 1.54 (t, 3H, $J=7.4$ Hz); ^{13}C NMR (125 MHz, CDCl_3) δ =153.93 (1C), 150.12 (1C), 145.22 (1C), 137.21 (1C), 128.09 (1C), 125.77 (1C), 124.76 (2C), 121.91 (1C), 121.08 (1C), 120.01 ((1C), 119.99 (2C), 111.26 (1C), 37.13 (1C), 13.29 (1C). ^{19}F NMR (CDCl_3 , 376 MHz): δ =-130.15- -130.17 (m, 1F), -130.22- -130.25 (m, 1F). FTIR (KBr, cm^{-1}) 1639.2, 1594.9, 1505.6, 1491.3, 1423.2, 1341.9, 1277.3, 1203.3, 1135.3, 1110.4, 1024.0, 972.0, 852.4, 773.3, 752.1, 653.8. HRMS (ESI): calcd for $\text{C}_{16}\text{H}_{13}\text{BF}_2\text{N}_4\text{O}_3$ Na, $[\text{M} + \text{Na}]^+$ 381.0946, found 381.0946.

4.3.7. *5-benzyl-3,3-difluoro-2-phenyl-3,5-dihydro-2H-[1,3,4,2]oxadiazaborinino[6,5-*

b]indol-4-ium-3-uide (compound **3g**). Orange solid. Yield 84%. Mp: 145-149 °C. ¹H NMR (500 MHz, CDCl₃): δ=7.89-7.86 (m, 3H), 7.48 (t, 2H, *J*=1.9 Hz), 7.45-7.28 (m, 8H), 7.17 (d, 1H, *J*=7.4 Hz), 5.27 (s, 2H). ¹³C NMR (125 MHz, CDCl₃): δ=153.14 (1C), 145.20 (1C), 136.28 (1C), 133.48 (1C), 129.30 (2C), 128.92 (2C), 128.72 (1C), 127.67 (2C), 127.11 (1C), 126.59 (1C), 125.03 (1C), 123.13 (1C), 121.58 (1C), 120.90 (1C), 118.95 (1C), 114.46 (1C), 111.62 (1C), 45.52 (1C). ¹⁹F NMR (CDCl₃, 376 MHz): δ=-130.96 (s, 1F), -131.02 (s, 1F). FTIR (KBr, cm⁻¹) 3060.5, 1634.0, 1508.1, 1458.1, 1266.7, 1183.4, 1133.0, 1023.8, 881.3, 757.9, 555.4. HRMS (ESI): calcd for C₂₁H₁₇BF₂N₃O, [M + H]⁺ 376.1427, found 376.1436.

4.3.8. 5- *p*-tert-butylbenzylindole -3,3-difluoro-2-phenyl-3,5-dihydro-2H-[1,3,4,2]oxadiazaborinino[6,5-*b*]indol-4-ium-3-uide (compound **3h**). Orange solid. Yield 83%. Mp: 152-153 °C. ¹H NMR (500 MHz, CDCl₃): δ=7.88-7.85 (m, 3H), 7.48-7.45 (m, 2H), 7.41-7.39 (m, 2H), 7.34-7.28 (m, 5H), 7.23-7.21 (m, 1H), 5.25 (s, 2H), 1.30 (s, 9H); ¹³C NMR (125 MHz, CDCl₃): δ=153.07 (1C), 151.81 (1C), 145.19 (1C), 136.34 (1C), 130.42 (2C), 128.98 (2C), 127.48 (2C), 127.10 (1C), 127.00 (1C), 126.52 (2C), 124.93 (1C), 123.16 (1C), 121.57 (1C), 120.84 (1C), 118.88 (1C), 114.40 (1C), 111.61 (1C), 45.16 (1C), 34.63 (1C), 31.31 (3C). ¹⁹F NMR (CDCl₃, 376 MHz): δ=-131.07 (s, 1F), -131.11 (s, 1F). FTIR (KBr, cm⁻¹) 2962.2, 1606.4, 1508.4, 1461.8, 1321.0, 1027.1, 887.1, 815.8, 763.7, 690.4, 557.3. HRMS (ESI): calcd for C₂₅H₂₅BF₂N₃O, [M + H]⁺ 432.2053, found 432.2061.

4.3.9. 5- *p*-tert-butylbenzylindole -3,3-difluoro-2-(4-methoxyphenyl)-3,5-dihydro-2H-

[1,3,4,2]oxadiazaborinino[6,5-b]indol-4-ium-3-uide (compound **3i**). Red solid. Yield 78%. Mp:156-157 °C. ¹H NMR (500 MHz, CDCl₃): δ=7.87-7.85 (m, 1H), 7.80 (d, 2H, *J*=9.0 Hz), 7.40- 7.38 (m, 2H), 7.34-7.28 (m, 4H), 7.22-7.20 (m, 1H), 6.99 (d, 2H, *J*=2.0 Hz), 5.24 (s, 2H), 3.88 (s, 3H), 1.30 (s, 9H); ¹³CNMR (125 MHz, CDCl₃): δ=158.94 (1C), 152.52 (1C), 151.70 (1C), 138.86 (1C), 135.94 (1C), 130.61 (1C), 127.41 (2C), 126.10 (2C), 124.69 (2C), 122.25 (2C), 121.59 (1C), 118.58 (1C), 114.23 (2C), 111.49 (2C), 55.57 (1C), 45.06 (1C), 34.60 (1C), 31.22 (3C). ¹⁹F NMR (CDCl₃, 376 MHz): δ=-131.61 (s, 1F), -131.67 (s, 1F). FTIR (KBr, cm⁻¹) 2941.0, 2738.5, 2678.7, 2491.6, 1606.4, 1499.9, 1427.1, 1323.9, 1248.8, 1176.3, 1026.1, 883.3, 833.1, 545.8. HRMS (ESI): calcd for C₂₆H₂₇BF₂N₃O₂, [M + H]⁺ 462.2159, found 462.2160.

4.3.10. 5- *p*-tert-butylbenzylindole -3,3-difluoro-2-(4-nitrophenyl)-3,5-dihydro-2H-[1,3,4,2]oxadiazaborinino[6,5-b]indol-4-ium-3-uide (compound **3j**). Orange solid. Yield 70%. Mp: 220-222 °C. ¹H NMR (500 MHz, CDCl₃) δ=8.31-8.29 (m, 2H), 7.99 (d, 2H, *J*=9.0 Hz), 7.91-7.89 (m, 1H), 7.42-7.38 (m, 4H), 7.31 (d, 2H, *J*=8.3 Hz), 7.27-7.24 (m, 1H), 5.25 (s, 2H), 1.31 (s, 9H); ¹³C NMR (125 MHz, CDCl₃) δ=154.12 (1C), 152.30 (1C), 145.32 (1C), 137.53 (1C), 129.74 (1C), 128.09 (1C), 127.58 (2C), 126.36 (2C), 125.76 (1C), 124.78 (2C), 124.43 (1C), 121.05 (1C), 120.13 (1C), 120.12 (1C), 119.81 (1C), 115.60 (1C), 112.15 (1C), 45.56 (1C), 34.68 (1C), 31.24 (3C). ¹⁹F NMR (CDCl₃, 376 MHz): δ=-130.08 (s, 1F), -131.12 (s, 1F). FTIR (KBr, cm⁻¹) 2964.1, 1594.9, 1544.7, 1504.2, 1490.4, 1423.2, 1306.2, 1262.7, 1169.0, 1154.7, 1108.3, 1029.8, 850.5, 752.1, 673.0, 437.8. HRMS (ESI): calcd for C₂₅H₂₃N₄O₃, [M -

$\text{BF}_2]^+$ 427.1770, found 427.1724.

Acknowledgement

We gratefully acknowledge the financial supported by the Natural Science Foundation of China (21176223) and the National Natural Science Foundation of Zhejiang (LY13B020016) and the Key Innovation Team of Science and Technology in Zhejiang Province (2010R50018).

References

- [1] (a) Harriman, A.; Mallon, L.J.; Stewart, B.; Ulrich, G.; Ziessel, R. *Ann Chem Pharm.* **2007**, 19, 3191-3198; (b) Cao, Q.; Xiao, S.Z.; Mao, M.F.; Chen, X.H.; Wang, S.; Li, L.; Zou, K. *J Organomet Chem.* **2012**, 717, 147-151; (c) Wang, D.F.; Liu, R.; Chen, C.; Wang, S.F.; Chang, J.; Wu, C.H.; Zhua, H.J.; Waclawik, E.R. *Dyes Pigments.* **2013**, 99, 240-249; (d) Luo, G.G.; Xia, J.X.; Fang, K.; Zhao, Q.H.; Wu, J.H.; Dai, J.C. *Dalton T.* **2013**, 42, 16268-16271.
- [2] (a) Descalzo, A. B.; Xu, H; Xue, Z.; Hoffmann, K.; Shen, Z.; Weller, M. G.; You, X.; Rurack, K. *Inorg. Chem.* **2010**, 49, 3730-3736; (b) Kaloudi-Chantzea, A.; Karakostas, N.; Raptopoulou, C. P.; Psycharis, V.; Saridakis, E.; Griebel, J.; Hermann, R.; Pistolis, G. J. *Am. Chem. Soc.* **2010**, 132, 16327-16329; (c) Kowada, T.; Yamaguchi, S.; Ohe, K. *Org. Lett.* **2010**, 12, 296-299; (d) Nastasi, F.; Puntoriero, F.; Campagna, S.; Olivierb, J. H.; Ziessel, R. *Phys. Chem. Chem. Phys.* **2010**, 12, 7392-7402; (e) Liu, J. Y.; El-Khouly, M. E.; Fukuzumi, S.; Ng, D. K. P. *Chem. Eur. J.* **2011**, 17, 1605-1613; (f) Gresser, R.; Hummert, M.; Hartmann, H.; Leo, K.; Riede, M. *Chem-Eur. J.* **2011**, 17, 2939-2947.
- [3] (a) Li, X.; Qian, S.; He, Q.; Yang, B.; Li, J.; Hu, Y. *Org. Biomol. Chem.* **2010**, 8, 3627-3630; (b) Sun, H.; Liu, S.; Ma, T.; Song, N.; Zhao, Q.; Huang, Wei. *New J. Chem.* **2011**, 35, 1194-1197; (c) Cheng, T.; Wang, T.; Zhu,

- W.; Chen, X.; Yang, Y.; Xu, Y.; Qian, X. *Org. Lett.* **2011**, 13, 3656-3659.
- [4] (a) Zhang, X.; Xiao, Y.; Qian, X. *Org. Lett.* **2008**, 10, 29-32; (b) Costela, A.; García-Moreno, I.; Pintado-Sierra, M.; Amat-Guerri, F.; Sastre, R.; Liras, M.; Arbeloa, F. L.; Prieto, J. B.; Arbeloa, I. L.J. *Phys. Chem. A* **2009**, 113, 8118-8124; (c) Ueno, Y.; Jose, J.; Loudet, A.; Pérez-Bolívar, C. Jr.; Burgess., *P. A. J. Am. Chem. Soc.* **2011**, 133, 51-55; (d) Lazarides, T.; McCormick, T. M.; Wilson, K. C.; Lee, S.; McCamant, D. W.; Eisenberg, R. *J. Am. Chem. Soc.* **2011**, 133, 350-364.
- [5] (a) Yogo, T.; Urano, Y.; Mizushima, A.; Sunahara, H.; Inoue, T.; Hirose, K.; Iino, M.; Kikuchi, K.; Nagano, T. *Proc. Natl. Acad. Sci. U.S.A.* **2008**, 105, 28-32; (b) Adarsh, N.; Avirah, R. R.; Ramaiah, D. *Org. Lett.* **2010**, 12, 5720-5723; (c) Awuah, S. G.; Polreis, J.; Biradar, V.; You, Y. *Org. Lett.* **2011**, 13, 3884-3887.
- [6] (a) Wu, W.; Guo, H.; Wu, W.; Ji, S.; Zhao, J. *J. Org. Chem.* **2011**, 76, 7056-7064; (b) Zhao, J.; Ji, S.; Guo, H. *RSC Adv.* **2011**, 1, 937-950; (c) Ji, S.; Guo, H.; Wu, W.; Wu, W.; Zhao, J. *Angew. Chem., Int. Ed.* **2011**, 50, 8283-8286.
- [7] (a) Peñ a-Cabrera, E.; Aguilar-Aguilar, A.; González-Domínguez, M.; Lager, E.; Zamudio-Vázquez, R.; Godoy-Vargas, J.; Villanueva-García, F. *Org. Lett.* **2007**, 9, 3985-3988; (b) Choi, S. H.; Kim, K.; Lee, J.; Do, Y.; Churchill, D. G. *J. Chem. Crystallogr.* **2007**, 37, 315-331; (c) Kim, K.; Jo, C.; Easwaramoorthi, S.; Sung, J.; Kim, D. H.; Churchill, D. G. *Inorg. Chem.* **2010**, 49, 4881-4894.
- [8] (a) Shirai, K.; Matsuoka, M.; Fukunishi, K. *Dyes Pigments*, **1999**, 42, 95-101; (b) Shirai, K.; Matsuoka, M.; Matsumoto, S.; Shiro, M. *Dyes Pigments*, **2003**, 56, 83-87; (c) Ooyama, Y.; Okamoto, T.; Yamaguchi, T.; Suzuki, T.; Hayashi, A.; Yoshida, K. *Chem-Eur J.* **2006**, 12, 7827-7838; (d) Park, S. Y.; Ebihara, M.; Kubota, Y.; Funabiki, K.; Matsui, M. *Dyes Pigments*. **2009**, 82, 259-267.
- [9] (a) Ulrich, G.; Ziesel, R.; Harriman, A. *Angew. Chem., Int. Ed.* **2008**, 47, 1184-1201; (b) Lee, J. S.; Kang, N.; Kim, Y. K.; Samanta, A.; Feng, S.; Kim, H. K.; Vendrell, M.; Park, J. H.; Chang, Y. T. *J. Am. Chem. Soc.* **2009**,

- 131, 10077-10082; (c) Benniston, A. C.; Copley, G. *Phys. Chem. Chem. Phys.* **2009**, 11, 4124-4131.
- [10] (a) Palma, A.; Tasiar, M.; Frimannsson, D. O.; Vu, T. T.; Meallet-Renault, R.; O' Shea, D. F. *Org. Lett.* **2009**, 11, 3638-3641; (b) Bellier, Q.; Pegaz, S.; Aronica, C.; Guennic, B. L.; Andraud, C.; Maury, O. *Org. Lett.* **2011**, 13, 22-25.
- [11] (a) Hepp, A.; Ulrich, G.; Schmechel, R.; von Seggern, H.; Ziessel, R. *Synth. Met.* **2004**, 146, 11-15; (b) Domercq, B.; Grasso, C.; Maldonado, J.-L.; Halik, M.; Barlow, S.; Marder, S. R.; Kippelen, B. *J. Phys. Chem. B* **2004**, 108, 8647-8651; (c) Zhang, G. Q.; Kooi, S. E.; Demas, J. N.; Fraser, C. L. *Adv. Mater.* **2008**, 20, 2099-2104; (d) Mao, M.F.; Xiao, S.Z.; Li, J.F.; Zou, Y.; Zhang, R.H.; Pan, J.R.; Dan, F.J.; Zou, K.; Yi, T. *Tetrahedron* **2012**, 68, 5037-5041;
- [12] (a) Song, Y.; Di, C.A.; Yang, X.D.; Li, S.P.; Xu, W.; Liu, Y.Q.; Yang, L.M.; Shuai, Z.G.; Zhang, D.Q.; Zhu, D.B. *J Am Chem Soc.* **2006**, 128, 15940-15941; (b) Zhou, Y.; Lei, T.; Wang, L.; Pei, J.; Cao, Y.; Wang, J. *Adv Mater.* **2010**, 22, 1484-1487; (c) Lu, L.; Yu, F.F.; Long, L.; Yu, J.N.; Wei, B.; Zhang, J.H.; Ichikawa, M. *Synthetic Met.* **2010**, 160, 2417-2421; (d) Liu, C.; Minari, T.; Lu, X.B.; Kumatani, A.; Takimiya, K.; Tsukagoshi, K. *Adv Mater.* **2011**, 23, 523-526; (e) Gholamrezaie, F.; Asadi, K.; Kicken, R.A.H.J.; Langeveld-Voss, B.M.W.; Leeuw, D.M.; Blom, P.W.M. *Synthetic Met.* **2011**, 161, 2226-2229.
- [13] (a) Wu, S.D.; Wang, X.Y.; Zhu, C.C.; Song, Y.J.; Wang, J.; Li, Y.Z.; Guo, Z.J. *Dalton T.* **2011**, 40, 10376-10382; (b) Tu, W.W.; Lei, J.P.; Wang, P.; Ju, H.X. *Chem Eur J.* **2011**, 17, 9440-9447; (c) Zhang, X.Q.; Zhang, X.Y.; Yang, B.; Hui, J.F.; Liu, M.; Chi, Z.G.; Liu, S.W.; Xu, J.; Wei, Y. *Polym Chem.* **2014**, 5, 318-322.
- [14] (a) Mishra, A.; Periasamy, N.; Patankar, M.P.; Narasimhan, K.L. *Dyes Pigments.* **2005**, 66, 89-97; (b) Zhao, J.; Yu, J.S.; Ma Z.; Li L.; Jiang, Y.D. *Synthetic Met.* **2011**, 161, 2417-2241; (c) Li, H.Y.; Chi, Z.Q.; Zhang, X.Q.; Xu, B.Q.; Liu, S.W.; Zhang, Y.; Xu, J.R. *Chem Commun.* **2011**, 47, 11273-11275; (d) Gao, C.H.; Zhou, D.Y.; Gu, W.; Shi, X.B.; Wang, Z.K.; Liao, L.S. *Organic Elect.* **2013**, 14, 1177-1182.

- [15] (a) Sun, F.; Zhang, G.; Zhang, D.; Xue, L.; Jiang, H. *Org Lett.* **2011**, 13, 6378-6381; (b) Benelhadj, K.; Massue, J.; Retailleau, P.; Ulrich, G.; Ziessel, R. *Org Lett.* **2013**, 15, 2918-2921.
- [16] Li, H.Y., Chi, Z.Q.; Zhang, X.Q.; Xu, B.Q.; Liu, S.W.; Zhang, Y.; Xu, J.R. *Chem Commun.* **2011**, 47, 11273-11275.
- [17] Zheng, J.; Huang, F.; Li, Y.J.; Xu, T.W.; Xu, H.; Jia, J.H.; Ye, Q.; Gao, J.R. *Dyes Pigments.* **2015**, 113, 502-509.
- [18] (a) Hehre, W.J.; Ditchfield, R.; Pople, J.A. *J. Chem. Phys.* **1972**, 56, 2257-2261; (b) Lee, C.; Yang, W.; Parr, R.G.; *Rev. Phys. B.* **1988**, 37, 785-789; (c) Becke, A.D. *J. Chem. Phys.* **1993**, 98, 5648-5652.
- [19] Frisch, M.J.; Trucks, G.W.; Schlegel, H.B.; Scuseria, G.E.; Robb, M.A.; Cheeseman, J.R.; Zakrzewski, V.G.; Montgomery Jr., J.A.; Stratmann, R.E.; Burant, J.C.; Dapprich, S.; Millam, J.M.; Daniels, A.D.; Kudin, K.N.; Strain, M.C.; Farkas, O.; Tomasi, J.; Barone, V.; Cossi, M.; Cammi, R.; Mennucci, B.; Pomelli, C.; Adamo, C.; Clifford, S.; Ochterski, J.; Petersson, G.A.; Ayala, P.Y.; Cui, Q.; Morokuma, K.; Malick, D.K.; Rabuck, A.D.; Raghavachari, K.; Foresman, J.B.; Cioslowski, J.; Ortiz, J.V.; Stefanov, B.B.; Liu, G.; Liashenko, A.; Piskorz, P.; Komaromi, I.; Gomperts, R.; Martin, R.L.; Fox, D.J.; Keith, T.; Al-Laham, M.A.; Peng, C.Y.; Nanayakkara, A.; Gonzalez, C.; Challacombe, M.; Gill, P.M.W.; Johnson, B.G.; Chen, W.; Wong, M.W.; Andres, J.L.; Head-Gordon, M.; Replogle, E.S.; Pople, J.A.; Gaussian 09, Gaussian Inc., Wallingford, CT, **2009**.
- [20] (a) Chen, Y.H.; Zhao, J.Z.; Guo, H.M.; Xi, L.J. *J Org Chem.* **2012**, 77, 2192-2206; (b) Găină, L.; Gal, E., Mătarângă-Popa, L., Porumb, D., Alina Nicolescu, A., Cristea, C., Silaghi-Dumitrescu, L. *Tetrahedron* **2012**, 68, 2465-2470.
- [21] Valeur, B.; *Molecular Fluorescence: Principles and Applications*, **2001**.
- [22] Chen, G.; Liu, B.; Tang, Y.; Deng, Q.; Hao, X.J. *Heterocycl Commun.* **2010**, 16, 25-32.
- [23] Hajare, R.A.; Gaurkhede, R.M.; Chinchole, P.P.; Chandewar, A.V.; Wandhare, A.S.; Karki, S.S. *Asian J Res Chem.* **2009**, 2, 289-291.